Supplemental Material for

Dual-Fullerene-Confined Single Transition Metal Atoms as High-Efficiency Catalysts for Hydrogen Evolution Reaction

Jingying Wei[a,b], Mingyang Shi[b], Kunyang Cheng[b], Jiguang Du[a,*]

[a] College of Physics, Sichuan University, Chengdu 610064, China

[b] Institute of Atomic and Molecular Physics, Sichuan University, Chengdu 610065, China

Table S1. Binding energy E_b(eV) for TM@$(C_{60})_2$ as well as other systems, B1(Å), B2(Å), B3(Å), B4(Å) is bond length between the TM atom and the adjacent C atom for TM@$(C_{60})_2$, and the sum of the covalent radius of the TM atom and C atom (r_c(TM)+r_c(C)) (Å).

species	E_b	B1	B2	B3	B4	r_c(M)+r_c(C)
Sc	−3.43	2.26	2.26	2.25	2.27	2.43
	−2.98[c]					
	−0.67[d]					
Ti	−3.94	2.09	2.08	2.08	2.09	2.33
	−1.58[a]					
	−1.30[b]					
	−3.09[c]					
	−2.22[d]					
V	−2.95	2.17	2.17	2.17	2.17	2.26
	−2.82[c]					
	−0.57[d]					
Cr	−2.15	2.19	2.19	2.12	2.12	2.12
	−0.18[a]					
	−3.24[c]					
	−1.16[d]					
Mn	−2.42	2.11	2.10	2.10	2.11	2.12
	−0.10[a]					

	−1.53[c]					
	−3.94[d]					
Fe	−2.39	2.16	2.18	1.95	1.95	2.05
	−0.66[a]					
	−0.85[b]					
	−2.08[c]					
	−4.30[d]					
Co	−3.55	2.13	2.11	1.92	1.93	1.99
	−1.20[a]					
	−2.64[c]					
	−3.46[d]					
Ni	−3.93	2.10	2.09	1.90	1.90	1.97
	−6.14[c]					
	−3.48[d]					
Cu	−2.35	2.05	2.06	2.06	2.05	2.05
	−3.46[c]					
	−3.39[d]					
Y	−3.66	2.55	2.53	2.55	2.53	2.63
Zr	−4.34	2.23	2.22	2.22	2.23	2.48
Nb	−3.97	2.13	2.14	2.14	2.13	2.37
Mo	−2.21	2.3	2.3	2.4	2.24	2.27
Tc	−3.12	2.23	2.23	2.22	2.23	2.20
Ru	−3.92	2.25	2.24	2.08	2.08	2.19
Rh	−4.11	2.26	2.25	2.06	2.06	2.15
Pd	−3.02	2.24	2.22	2.08	2.08	2.12
	−1.08[b]					
Ag	−1.28	2.25	2.25	2.25	2.26	2.18
Hf	−4.81	2.16	2.17	2.17	2.17	2.48
Ta	−4.93	2.12	2.12	2.13	2.12	2.43

W	−4.01	2.24	2.24	2.24	2.24	2.35
Re	−3.52	2.24	2.22	2.08	2.08	2.24
Os	−4.03	2.18	2.20	2.05	2.04	2.17
Ir	−4.95	2.22	2.22	2.05	2.05	2.14
Pt	−4.97	2.22	2.22	2.04	2.04	2.09
Au	−2.20	2.16	2.16	2.15	2.16	2.09
	−0.10[b]					

[a]ref[1]
[b]ref[2]
[c]ref[3]
[d]ref[4]

Table S2. Magnetic moment M (μ_B), Bader charge of metallic atoms (Q_{TM*}) and neighboring carbon atoms (Q_{C*}) in TM@$(C_{60})_2$ complexes.

		Bader Charge (|e|)	
species	M	Q_{TM*}	Q_{C*}
Sc	0.76	1.352	−0.087
Ti	0.00	1.402	−0.096
V	2.86	1.110	−0.108
Cr	4.00	0.871	−0.097
Mn	4.34	0.713	−0.106
Fe	2.02	0.642	−0.064
Co	1.00	0.630	−0.073
Ni	0.00	0.407	−0.081
Cu	0.00	0.335	−0.089
Y	0.00	1.727	−0.086
Zr	0.00	1.793	−0.095
Nb	1.00	1.372	−0.104
Mo	4.00	0.735	−0.113
Tc	3.62	0.846	−0.105
Ru	2.00	0.608	−0.114
Rh	1.00	0.352	−0.123
Pd	0.00	0.266	−0.082
Ag	0.00	0.334	−0.088
Hf	0.00	1.732	−0.079
Ta	1.00	1.668	−0.088
W	2.00	0.857	−0.117
Re	3.00	1.016	−0.037
Os	0.00	0.724	−0.064
Ir	1.00	0.599	−0.072
Pt	0.00	0.354	−0.081
Au	0.00	0.499	−0.090

Table S3. The adsorption energy ΔE_{ads}(eV), Gibbs free energy ΔG_{H*}(eV) of studied species for the hydrogen evolution reaction, the exchange current (Log(i_0/(Acm^{-2}))), magnetic moment M(μ_B) and the Bader charge of the H atom, the TM atom, and the C atom (Q_{H*}, Q_{TM*}, Q_{C*}) in H adsorbed TM@$(C_{60})_2$ complexes.

					Bader Charge (|e|)		
spieces	ΔE_{ads}	ΔG_{H*}	Log(i_0)	M	Q_{H*}	Q_{TM*}	Q_{C*}
Sc	−0.119	0.067	−1.157	0.00	−0.567	1.494	−0.087
Ti	0.007	0.223	−3.718	0.99	−0.449	1.283	−0.096
V	0.061	0.270	−4.504	1.87	−0.459	1.160	−0.105
Cr	0.210	0.416	−6.946	3.00	−0.445	1.012	−0.096
Mn	0.246	0.467	−7.809	4.00	−0.336	0.944	−0.106
Fe	−0.407	−0.188	−3.144	0.06	−0.302	0.870	−0.064
Co	−0.043	0.218	−3.635	0.00	−0.288	0.716	−0.073
Ni	0.487	0.702	−11.725	0.09	−0.266	0.501	−0.081
Cu	0.533	0.760	−12.694	0.00	−0.308	0.605	−0.089
Y	−0.388	−0.218	−3.645	0.00	−0.643	1.851	−0.086
Zr	−0.272	−0.063	−1.093	0.93	−0.620	1.952	−0.095
Nb	−0.690	−0.439	−7.331	0.00	−0.542	−0.208	−0.104
Mo	−0.513	−0.333	−5.561	3.00	−0.452	1.174	−0.113
Tc	−0.772	−0.544	−9.092	2.00	−0.341	1.064	−0.105
Ru	−0.545	−0.325	−5.431	0.00	−0.263	0.774	−0.114
Rh	−0.741	−0.486	−8.117	0.00	−0.224	0.474	−0.123
Pd	0.688	0.888	−14.841	0.14	−0.168	0.344	−0.082
Ag	0.877	1.051	−17.560	0.00	−0.452	0.422	−0.088
Hf	0.182	0.472	−7.877	0.00	−0.490	1.782	−0.079
Ta	−0.247	0.040	−0.756	0.00	−0.433	1.238	−0.088
W	−0.705	−0.509	−8.500	2.97	−0.444	1.122	−0.113
Re	−0.546	−0.288	−4.815	0.59	−0.404	1.248	−0.055
Os	−1.092	−0.808	−13.490	1.00	−0.371	1.200	−0.064
Ir	−1.244	−0.976	−16.304	0.00	−0.409	0.605	−0.072
Pt	0.153	0.375	−6.256	0.00	−0.302	0.603	−0.081
Au	0.326	0.596	−9.957	0.00	−0.247	0.575	−0.090

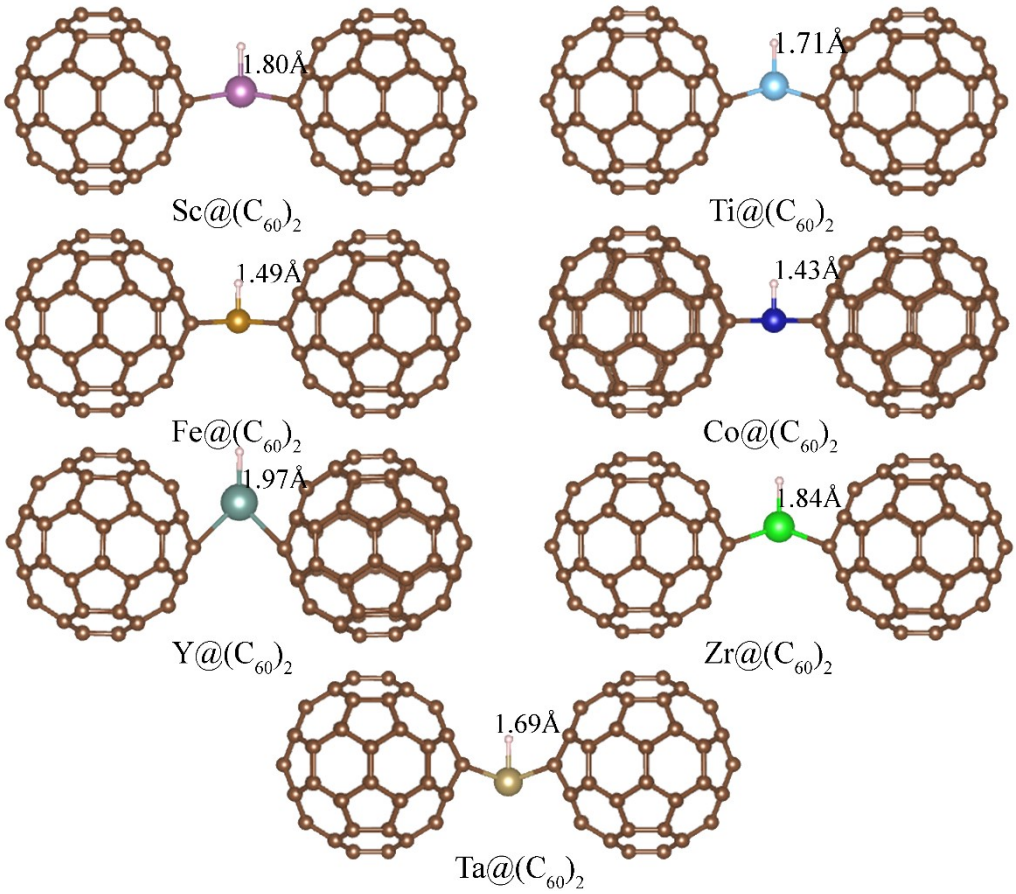

Figure S1. The relaxed configurations of TM@$(C_{60})_2$ upon H adsorption for the species showing excellent Gibbs free energy (ΔG_{H*}), and bond length between H and the TM atom is also depicted.

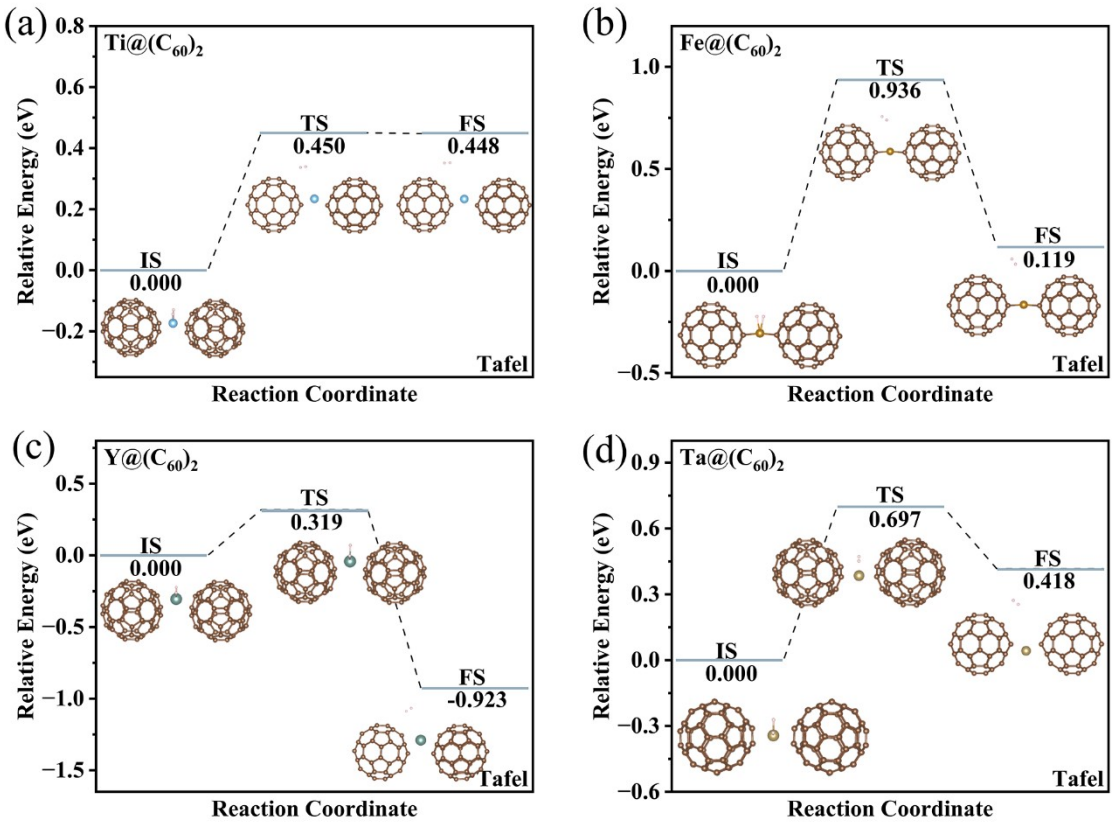

Figure S2. (a) $Ti@(C_{60})_2$, (b) $Fe@(C_{60})_2$, (c) $Y@(C_{60})_2$, (d) $Ta@(C_{60})_2$ energy barriers under the Tafel pathway.

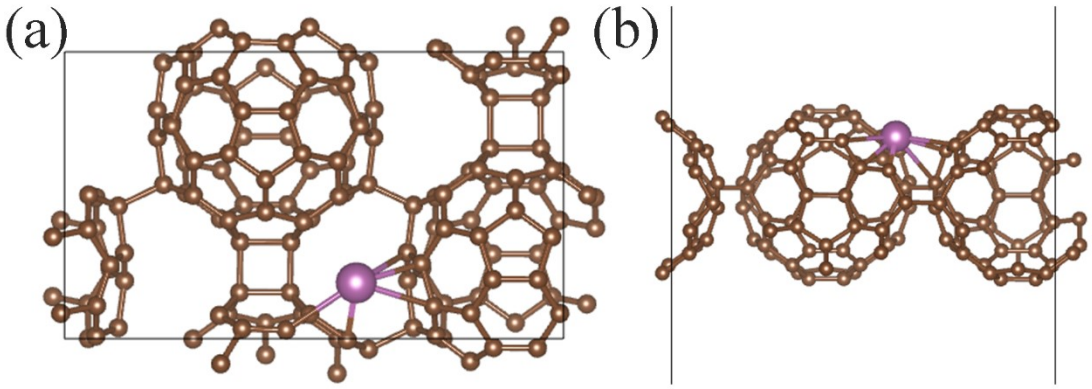

Figure S3. Structural representation of single TM atom doping in the 2D qHP C_{60} monolayer. (a) top view, (b) side view.

Table S4. The binding energy E_b and Gibbs free energy values ΔG_{H^*} of TM@$(C_{60})_2$ and TM@qHP C_{60}.

	E_b		ΔG_{H^*}	
	TM@$(C_{60})_2$	TM@qHP C_{60}	TM@$(C_{60})_2$	TM@qHP C_{60}
Sc	−3.430	−4.730	0.067	0.120
Ti	−3.939	−4.913	0.223	−0.120
Fe	−2.389	−4.223	−0.188	0.511
Co	−3.548	−4.544	0.218	0.199
Y	−3.660	−5.049	−0.218	0.239
Zr	−4.342	−5.868	−0.063	−0.232
Ta	−4.930	−6.089	0.040	−0.840
Pt	−4.969	−5.162	0.375	0.510

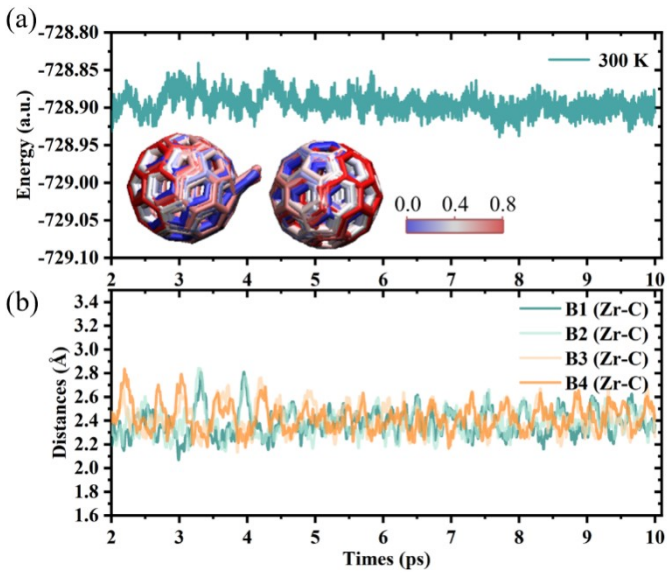

Figure S4. (a) Energy variation of Zr@$(C_{60})_2$ over the 10 ps simulation at 300 K. Insets show structural snapshots taken every 500 fs, with color coding from red to white to blue indicating the progression of time. (b) Variation of bond distances between Zr and its four neighboring C atoms during the 10 ps simulation.

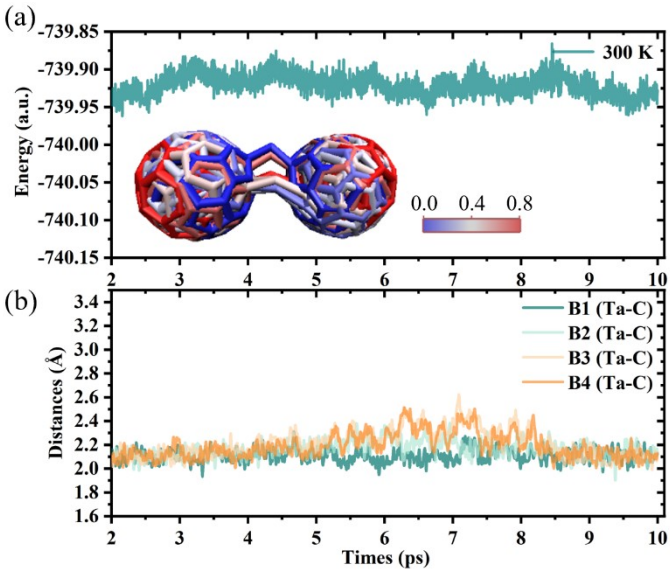

Figure S5. (a) Energy variation of Ta@$(C_{60})_2$ over the 10 ps simulation at 300 K. Insets show structural snapshots taken every 500 fs, with color coding from red to white to blue indicating the progression of time. (b) Variation of bond distances between Ta and its four neighboring C atoms during the 10 ps simulation.

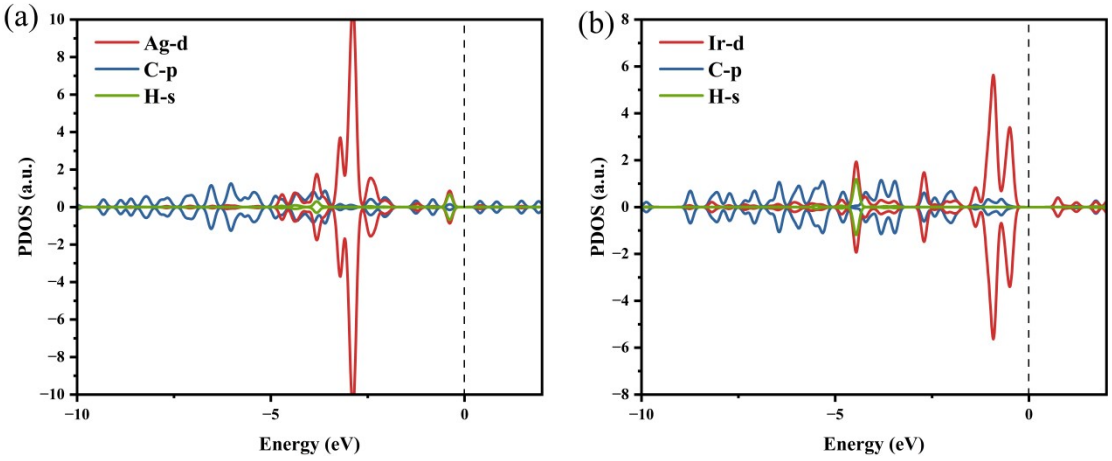

Figure S6. PDOS of the d−orbitals of the TM, p−orbitals of carbon C atoms, and the s−orbitals of H in hydrogen adsorbed species (a) Ag@$(C_{60})_2$ and (b) Ir@$(C_{60})_2$.

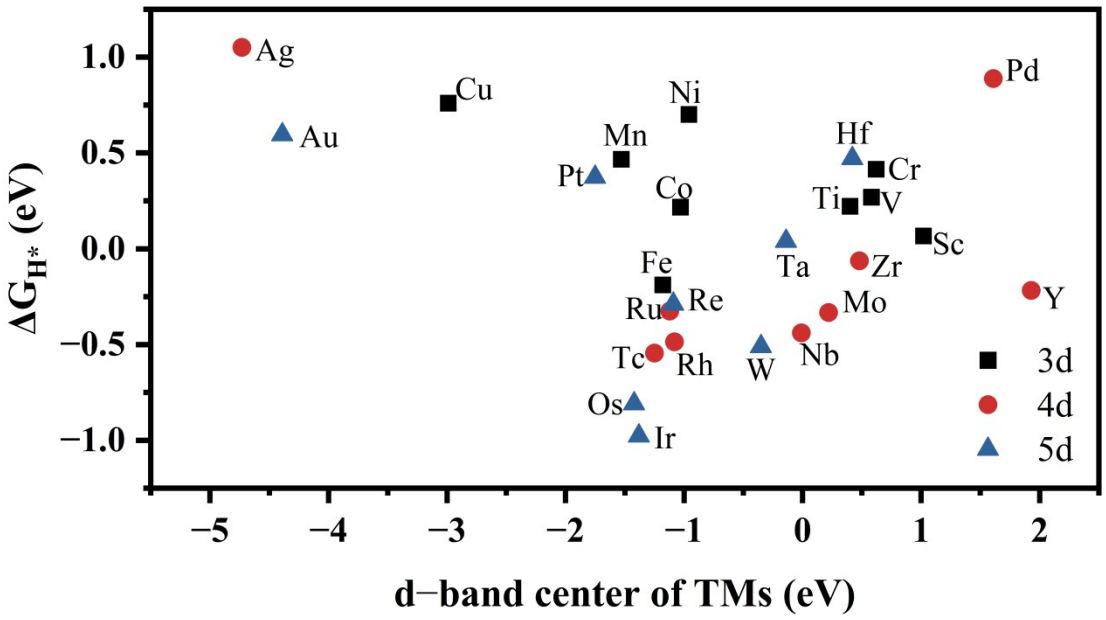

Figure S7. Relationship plot of the d−band center of TM@$(C_{60})_2$ versus Gibbs free energy ΔG_{H*}.

Reference

(1) Sevinçli, H.; Topsakal, M.; Durgun, E.; Ciraci, S. Electronic and Magnetic Properties of 3 d Transition-Metal Atom Adsorbed Graphene and Graphene Nanoribbons. *Phys. Rev. B* **2008**, *77* (19), 195434.

(2) Chan, K. T.; Neaton, J. B.; Cohen, M. L. First-Principles Study of Metal Adatom Adsorption on Graphene. *Phys. Rev. B* **2008**, *77* (23), 235430.

(3) Sarfaraz, S.; Yar, M.; Sheikh, N. S.; Bayach, I.; Ayub, K. Transition Metal-Doped C_{20} Fullerene-Based Single-Atom Catalysts with High Catalytic Activity for Hydrogen Dissociation Reaction. *ACS Omega* **2023**, *8* (15), 14077–14088.

(4) Sarfaraz, S.; Yar, M.; Ayub, K. The Electronic Properties, Stability and Catalytic Activity of Metallofullerene (M@C60) for Robust Hydrogen Evolution Reaction: DFT Insights. *Int. J. Hydrog. Energy* **2024**, *51*, 206–221.